Binding of Anionic Ligands to Peptic Fragments of Bovine Serum Albumin

HERMAN MEISNER

Department of Pharmacology, Case Western Reserve University, School of Medicine, Cleveland, Ohio 44106

SUMMARY

MEISNER, H. Binding of anionic ligands to peptic fragments of bovine serum albumin. *Mol. Pharmacol.* **18**: 224–229 (1980).

The binding of anionic ligands was determined in fragments of bovine serum albumin prepared by pepsin digestion. The two fragments were the —NH₂ terminal (amino acids 1–306) and the —COOH terminal half (amino acids 307–582), originally described by T. King [*Arch. Biochem. Biophys.* **156**: 509–520 (1973)]. Ligand binding and competitive interactions were described by a Scatchard model having multiple independent sites. Equilibrium partitioning at 37°C showed that ^{14}C-palmitate was bound to the —COOH terminal fragment (P-A) at one high-affinity site, $k_1 = 5.2 \times 10^6$ M^{-1}, while the —NH₂ terminal fragment (P-B) bound up to 4 mol with a lower affinity. The weaker binding ligands octanoate and chlorophenoxyisobutyrate (CPIB) displaced ^{14}C-palmitate competitively from fragments P-A and P-B, respectively, with apparent competition constants (k_i') 10^{-1} less than the respective association constants (k_i). Fragment P-A contained 0.4–0.8 high-affinity sites for ^{14}C-CPIB and ^{3}H-ANS, with a k_1 of 10^5 M^{-1}, and fragment P-B bound these ligands at several low-affinity sites $(k_i \cong 10^3$ M$^{-1})$. The binding curve of ^{3}H-ANS to reconstituted albumin, prepared by mixing equimolar amounts of P-A and P-B, was greater than to either peptic fragment. The profile equaled that obtained by summing the affinity constants of P-A and P-B. It is concluded that P-A is the fragment with a strong binding site for anionic ligands, but few if any weak sites, while P-B contains multiple weak sites and no strong sites. These data were explained in terms of a model with initially independent sites of unequal affinity for the ligand.

INTRODUCTION

Albumin is a plasma protein that adsorbs numerous organic ligands, from bilirubin and long-chain free fatty acids to anionic and basic drugs, with affinity constants of 10^4–10^7 M^{-1} (1). Based on amino acid sequence (2), the molecule is thought to consist of three domains, stabilized by disulfide bonds (3). The protein has been hydrolyzed into smaller fragments by cyanogen bromide (4), pepsin (5–7), and trypsin (8–10) digestion. Pepsin digestion of bovine serum albumin (BSA)[1] at pH 3.7 yields predominantly two fragments (4): P-B, the —NH₂ terminal half consisting of amino acids 1–306; and P-A, the —COOH terminal fragment containing amino acids 307–582.

The binding of various physiological ligands and drugs

[1] Abbreviations used: BSA, bovine serum albumin; CPIB, chlorophenoxyisobutyrate; ANS, 8-anilino-1-naphthalenesulfonate; FFA, free fatty acids; P-A and P-B, peptic fragments A and B, designated by King (4).

to BSA has been investigated extensively (1, 11), but less is known about the interaction of proteolytic fragments with these molecules. It is believed, however, that fragment P-A contains the sites for long-chain free fatty acids (4, 12) and octanoate (4), while the NH₂ terminus contains sites for bilirubin (10, 13) and long-chain FFA (4, 10). Quantitative measurement of the interaction between ligands and these fragments has been limited (4), although such a study may clarify the nature and location of ligand binding sites. In the previous paper (14), we have developed the equations to enable us to compare quantitatively the interaction between two ligands at multiple sites on a protein. The purpose of this paper is to compare quantitatively the binding of anionic ligands of differing affinities to fragments produced by peptic digestion.

METHODS

Limited pepsin digestion of BSA (Armour, crystallized) was carried out as described (4, 7, 15). Basically, half-cystinyl nondefatted BSA, prepared by reacting with L-

cystine, was digested with pepsin at a 500:1 (w/w) ratio, in 0.2 M ammonium formate buffer, pH 3.7. At this pH, BSA changes into a partially expanded molecule, a process that is reversed upon raising the pH (16). Between 3 and 5 mM octanoate was added initially to prevent further degradation of the main fragments (4). We have also used oleate or chlorophenoxyisobutyrate to protect albumin from extensive proteolysis, with similar results (Meisner, unpublished). After 20 min at 23°C, the digestion was stopped by adjusting the pH to 8.0 with Tris, and the solution was stirred for 1 h, concentrated by ultrafiltration through a UM-10 membrane, and extensively dialyzed against 0.23 M ammonium formate, pH 3.0. The digest was applied at 4°C to a Sephadex G-100 column, 5 × 130 cm, previously equilibrated with pH 3.0 ammonium formate and eluted at 20 ml/h. The column effluent was monitored at 280 nm, and the tubes corresponding to the 25,000–45,000 molecular weight fragments were pooled. After concentration and dialysis vs 0.1 M Tris, pH 8, the two fragments were separated on a DEAE column (0.9 × 25 cm), using a linear gradient of 300 ml 0.1 M Tris, pH 8.0, and 300 ml 0.1 M Tris, pH 8.0–0.15 M NaCl. The two major fragments were concentrated, dialyzed against distilled water, and stored at −60°C. Molecular weight determination of both fragments was carried out by polyacrylamide–SDS slab gel electrophoresis according to Laemmli et al. (17), with 15% gels crosslinked with 0.1% BIS.

Circular dichroism spectra were measured with a JASCO J-20 spectropolarimeter, at 0.3 mg protein/ml, in pH 7.4, 0.1 M phosphate buffer, using a pathlength of 0.1 cm, at scale settings of 0.002–0.005. The instrument was calibrated with d-10-camphorsulfonic acid prior to each experiment. The percentages of α, β, and random structures were calculated from mean residue ellipticities observed in the 250- to 200-nm region, by comparison with the ellipticities found by Chen et al. (18). A least-squares regression program was used to calculate the final values of α, β, and random structures from 13 equally weighted wavelength pairs, between 240 and 207 nm.

Determination of —NH$_2$ and —COOH terminal groups of BSA and fragments P-A and P-B was carried out with dansyl chloride (19). For —NH$_2$ terminal analysis, the desiccated hydrolysate from the 105°C extraction was reextracted with water-saturated ethyl acetate to remove dansylated peptide impurities, which interfered with the amino acid separation. In the —COOH terminal determination, fragment P-A was reacted for 10 and 20 min with carboxypeptidase A at a ratio of 1:40 (w/w), enzyme: peptide, in 0.2 M N-ethylmorpholine acetate buffer, pH 8.5. BSA and fragment P-B were digested with a 1:10 (w/w) mixture of carboxypeptidases A and B for 15 to 30 min (20) at the same enzyme:peptide ratio. After quenching with acetic acid and evaporating slowly, dansylation of the free amino acids was carried out, omitting the hydrolysis step. The sample and dansyl-amino acid markers were spotted on both sides of polyamide sheets and separated as described (19) in the three solvent systems.

The equations used to describe ligand binding to a protein having multiple independent sites is detailed in the preceding paper (14). When a competitive ligand was included, the equation of Scatchard (21) was coupled to a model describing classical competition between two ligands for a single binding site:

$$\bar{\nu}_A = \sum k_i(A)/[1 + k_i(A) + k_i'(C)] \qquad [1]$$

and

$$\bar{\nu}_C = \sum k_i'(C)/[1 + k_i'(C) + k_i(A)], \qquad [2]$$

where $\bar{\nu}_A$ and $\bar{\nu}_C$ are the moles of ligand (A) and competitor (C), respectively, bound per mole of albumin, and k_i and k_i' are the affinity constants for A and C (14). In cases where one strong site and multiple weak sites exist, the equations were simplified as described (14). The data were then fit by a weighted nonlinear least-squares analysis, using a Univac 1108 computer, to obtain simultaneously the set of ligand or ligand–competitor association constants that gives the best fit to the data. This analysis is unique in that it accounts for variation in free competitor concentration as a function of ligand concentration. The constants obtained were used to simulate binding profiles of ligands on a Hewlett–Packard 9815 A calculator and 9862 A plotter. Further details are found in the preceding paper (14).

Synthesis of [2-^{14}C]chlorophenoxyisobutyrate was performed as described previously (22). The identity of ^{14}C-CPIB was verified by NMR spectroscopy at 270 MHz (Brucker Instrument Co.), with unlabeled CPIB synthesized in an identical manner as the radioisotopic drug. The product was at least 97% pure by thin-layer chromatography in methylcyclohexane–acetone–acetic acid (70:30:1, v/v) and radio high-performance liquid chromatography. The specific activity was 4613 dpm/nmol. Unlabeled monomer ANS was prepared as described (14); ^{3}H-ANS was provided by Drs. Hans Cahnmann and Harold Edelhoch, National Institute of Arthritis, Metabolism and Digestive Diseases, NIH (23), and had a specific activity of 23,400 dpm/nmol.

Equilibrium partitioning, using hexane as the organic phase, and equilibrium dialysis were carried out with 0.05–0.1 mM protein, pH 7.45, at 37°C for 16 h in a shaking water bath, as previously described (14, 24, 25). ^{14}C-Palmitate binding was determined by equilibrium partitioning, while ^{3}H-ANS and ^{14}C-CPIB binding was measured by equilibrium dialysis. The recovery of ^{3}H-ANS and ^{14}C-CPIB was 100%, with less than 2% bound to the membrane, while ^{14}C-palmitate recovery was proportional to the concentration. The mathematical analysis accounted for this variability. Samples were counted for radioactivity by liquid scintillation, using a solution of 0.4% 2,5-diphenyloxazole in 2:1 toluene–Triton X-100, correcting for quenching by the channels ratio method.

Endogenous long-chain free fatty acids (FFA) bound to albumin and fragments were measured by the ^{63}Ni method (26). FFA were removed from whole albumin, when required, by the activated charcoal method at pH 3.0 (27).

Chemicals. Crystallized BSA was obtained from Armour Pharmaceutical Co., Kankakee, Ill.; Sephadex G-100 from Pharmacia Fine Chemicals, Piscataway, N.J.; DEAE-cellulose (DE-32) from Whatman; pepsin, 2× crystallized, from Sigma; and [1-^{14}C]palmitate from New England Nuclear Corp., Boston, Mass.

RESULTS

Characterization of peptic fragments. Circular dichroism of fragments produced by pepsin digestion of BSA show that most of their secondary structure is retained (Table 1), although the α-helical content of fragment P-A falls from 57 to 48%, and fragment P-B drops to 42%. The lower percentage of α-helix in peptic fragments has been found by other investigators as well (10, 28). When P-A and P-B were mixed in equimolar amounts to "reconstitute" the whole molecule (12), the circular dichroic spectrum was unchanged. End-group analyses show the presence of phenylalanine and aspartate at the NH_2 terminus of P-A and P-B, respectively. Fragment P-A contains alanine and fragment P-B contains aspartate at the —COOH end. These observations are consistent with the work of other groups (4, 7), confirming that fragment P-A represents amino acids 307–582, and P-B consists of amino acids 1–306. Slab gel electrophoresis in 0.1% SDS showed no albumin present in peptic fragments and negligible quantities of low molecular weight material (data not shown). The molecular weight was 28,700 for P-A and 36,500 for P-B, which is slightly higher than reported elsewhere for the —NH_2 fragment (4, 10). The FFA content of defatted BSA and both fragments was between 0.08 and 0.11 mol/mol protein, which compares to 0.80 for nondefatted BSA. Evidently, the procedure for isolation of fragments P-A and P-B removes most of the endogenous long-chain FFA, an important consideration in the studies that follow.

Palmitate binding. A comparison of the binding of ^{14}C-palmitate to albumin, P-A, and P-B is shown in Fig. 1. The solid lines represent computer-derived best fits to the data, using affinity constants listed in the inset, Fig. 1. The affinity of the fragments for palmitate is less than the binding affinity to albumin and may be related to the lower α-helical content. Palmitate binding to fragment P-A was analyzed in terms of a coefficient model (14). Fragment P-A retains a higher-affinity primary binding site for palmitate ($n_1 = 0.8$, $k_1 = 8.0 \times 10^6$ M^{-1}) than does P-B ($n_1 = 1$, $k_1 = 2 \times 10^6$ M^{-1}), although the differences in affinity between the two fragments for palmitate is small. The number and association constants of second-
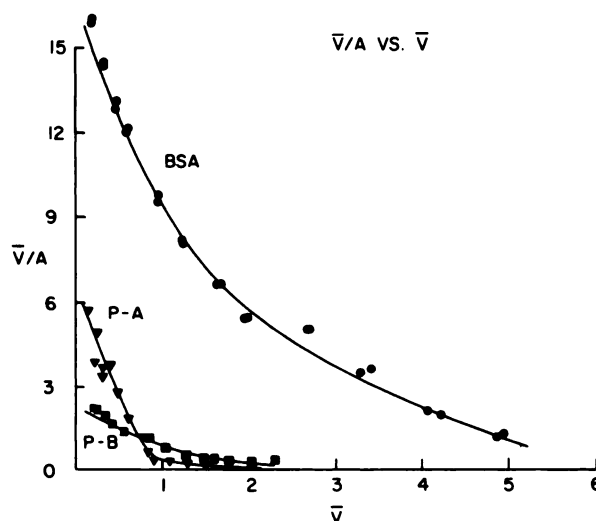

FIG. 1. *Binding of ^{14}C-palmitate to albumin and fragments P-A and P-B*

Solid lines represent a simulation of the data, using k_i values shown in Table 2. Ordinate, bound/free palmitate ($\times 10^6$ M); abscissa, moles ^{14}C-palmitate bound/mole protein.

ary sites for palmitate in P-A are low, of the order of 6 $\times 10^4$ M^{-1}, and it was not possible to bind more than 1.5 mol of the ligand to this fragment. Fragment P-B retains up to three sites, with affinities between 2 $\times 10^5$ and 2 $\times 10^6$ M^{-1}.

The interaction of weakly bound ligands with ^{14}C-palmitate binding to peptic fragments was examined by equilibrium partitioning (Figs. 2 and 3). The ligand shown competing with ^{14}C-palmitate for fragment P-A is octanoate (Fig. 2), and for fragment P-B the competitor is chlorophenoxyisobutyrate (CPIB) (Fig. 3). Both CPIB and octanoate can displace palmitate apparently competitively, as indicated by the computer fits (solid lines). The inset, Fig. 3, indicates that the competitor constant for CPIB is of the order of 10^3 M^{-1}, which is considerably lower than the k_1 of CPIB for whole albumin (22) but similar to the k_1 of CPIB with P-B (Fig. 4). The k_1 of octanoate to fragment P-A was not measured.

CPIB binding. The binding pattern of ^{14}C-CPIB to fragment P-A and P-B (Fig. 4) indicates that a high-affinity site is retained in P-A, but is not present in P-B. The association constants (see inset) obtained by the computer fit to the coefficient model show that the number of high-affinity binding sites for CPIB/mol of fragment A is only 0.4, with an affinity of 4.4 $\times 10^4$ M^{-1}. Although not shown, palmitate displaced ^{14}C-CPIB competitively from P-A, with a k_1' of 1.5 $\times 10^7$ M^{-1} for the high-affinity site. This corresponds well with the k_1 of palmitate of 8.8 $\times 10^6$ M^-; to P-A (fig. 2). The presence of fewer than one binding site for all the ligands tested per mole of fragment P-A may be due to either endogenous FFA or nonbinding fragments. Since endogenous FFA concentration is less than 0.1 mol/mol protein, it is more likely that a certain percentage of peptic fragment P-A does not bind the ligands. The association constants of ^{14}C-CPIB with fragment P-B are rather low, 0.6 $\times 10^3$ to 0.4 $\times 10^3$ M^{-1}, but represent the first quantitative estimates of the affinity constants for the drug to the

TABLE 1

Secondary structure, carboxyl- and amino-terminal sequences, and free fatty acid content of bovine albumin and peptic fragments from bovine albumin

Protein	Circular dichroism		—COOH terminal residue[b,c]	—NH_2 terminal residue[c]	mol FFA[d]/ mol protein
	% α	% β			
BSA	57[a]	17[a]	Ala	Asp	0.08
P-A	48	14	Ala	Phe	0.08
P-B	42	22	Asp	Asp	0.11
(P-A) + (P-B)[e]	43	18	n.d.[f]	n.d.	n.d.

[a] Calculated from circular dichroism spectra.

[b] Determined by carboxypeptidases A and B, followed by dansyl chloride.

[c] Dansyl chloride.

[d] ^{63}Ni analysis of long-chain FFA.

[e] Fragments P-A and P-B were mixed at a 1:1 molar ratio, pH 7.4.

[f] Not determined.

$\bar{V}/A$ VS. $\bar{V}$

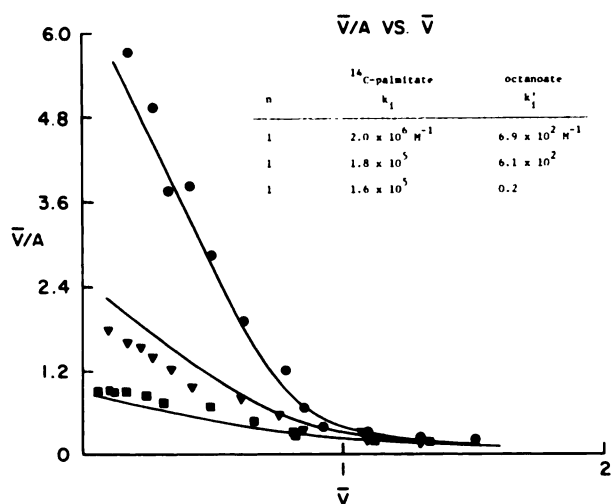| n	^{14}C-palmitate k_i	octanoate k_i'
1	$2.0 \times 10^6 \, M^{-1}$	$6.9 \times 10^2 \, M^{-1}$
1	1.8×10^5	6.1×10^2
1	1.6×10^5	0.2

FIG. 2. *Displacement of ^{14}C-palmitate by octanoate in fragment P-A*

Solid lines represent the best-fit simulations, using the computer-derived k_i and k_i' values shown in the inset. Triangles, 0.5 mM octanoate; squares, 2 mM octanoate. Ordinate, bound/free palmitate ($\times 10^6$ M); abscissa, moles ^{14}C-palmitate bound/mole P-A.

—NH$_2$ fragment. In this experiment, it was not possible to bind more than 1 (P-A) or 2 (P-B) mol CPIB/mol protein, compared to 9–10 mol bound to the native, intact albumin (22).

ANS binding. The binding of ^3H-ANS to fragment P-A and P-B is shown in Fig. 5. In the case of P-A, it was again necessary to use the coefficient model (14), with n_1 = 0.8, to obtain the best fit to the data. The computer-derived best fit (solid lines) yields association constants (see inset) suggesting that the high-affinity site is retained in the —COOH terminal fragment P-A (k_1 = 3.5 $\times 10^5$ M^{-1}), but is not present in P-B, the —NH$_2$ terminal fragment (k_1 = 5.3 $\times 10^4$ M^{-1}). Fragment P-B, however, has several low-affinity sites for ANS. The filled circles in Fig. 5 represent the binding of ^3H-ANS to equimolar mixtures of P-A and P-B. The dashed line is a computer simulation, representing a simple summation of $\bar{v}$ for k_i (P-A) and k_i (P-B) at each free ligand concentration. The experimentally derived line is only slightly greater than the simulated curve, suggesting that a simple summation of binding sites is adequate to account for most ANS binding to "reconstituted" BSA. Although for the purpose of the Scatchard analysis, it is unnecessary to place the constants in any particular order, based on binding data, we are assuming that fragments P-A and P-B represent the strong and weak sites, respectively.

Fluorescence titrations of increasing concentrations of monomer ANS were carried out with half-cystinyl BSA and the peptic fragments (Fig. 6). At 1 μM protein, the maximal fluorescence with BSA was reached at an ANS: protein ratio of approximately 40. The —NH$_2$ and —COOH terminal fragments were 23 and 14% as effective, respectively, as BSA with regard to the maximal fluorescence of ANS. A 1:1 mixture of fragments P-A and P-B showed a fluorescence roughly equal to the sum of both fragments. It was not possible to obtain association constants from the fluorescence data, despite linear double-reciprocal plots, because the free ANS concentra-

tion could not be determined. The greater fluoresence enhancement of ANS bound to P-B than to P-A is not related to the higher-affinity of fragment P-A for ^3H-ANS (Fig. 5) and is consistent with our companion study (14), showing that fluoresence cannot be quantitated to affinity constants.

Table 2 compares the association constants for the binding of palmitate, ANS, and CPIB to BSA and peptic fragments P-A and P-B. Long-chain FFA, as represented by ^{14}C-palmitate, appear to retain high-affinity sites in both fragments. However, the differences in affinity between "strong" and "weak" binding sites on BSA for palmitate are small, between 8 $\times$ 10^6 and 2 $\times$ 10^6 M^{-1}. The association constants of palmitate in fragment P-B may therefore represent the secondary binding sites. As estimated from the k values, the ligands CPIB and ANS show a twofold reduction in binding to fragment P-A, but a 10- to 200-fold loss in binding to fragment P-B. The association constants of CPIB and ANS to P-B are similar to the secondary site constants of these ligands to intact albumin.

DISCUSSION

Location of anionic ligand binding sites. The studies reported here, involving several anions having differing affinities toward BSA, emphasize that the —COOH terminal half of BSA contains the primary binding site for these ligands. This is true not only for tightly bound ligands such as long-chain FFA, but also for weakly bound octanoate, ANS, and CPIB. The —NH$_2$ terminal fragment P-B retains a weaker affinity, but more numerous sites, toward all these ligands. Similar views have been expressed by others (12) for FFA. However, the use of radioactively labeled CPIB and ANS in this study has demonstrated clearly that fragments P-A and P-B contain the strong and weak sites, respectively, for less strongly bound ligands as well. It may be argued that the low affinity of ligands toward fragment P-B is a reflection of the loss of secondary structure, as revealed in the α-
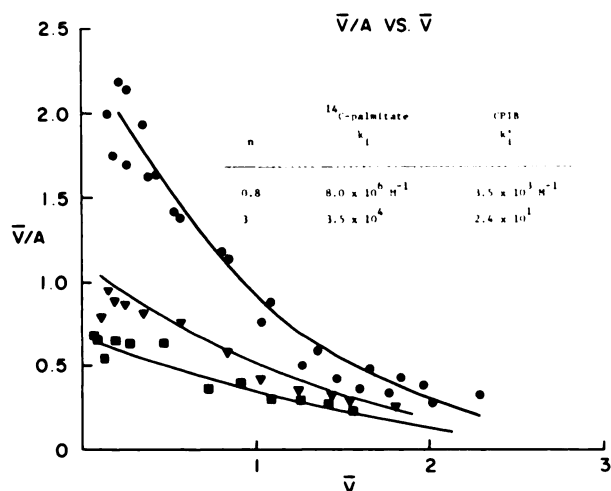

$\bar{V}/A$ VS. $\bar{V}$

n	^{14}C-palmitate k_i	CPIB k_i'
0.8	$8.0 \times 10^6 \, M^{-1}$	$3.5 \times 10^3 \, M^{-1}$
1	1.5×10^4	2.4×10^1

FIG. 3. *Displacement of ^{14}C-palmitate by CPIB in fragment P-B*

Solid lines represent a simulation of the data, based on simultaneous computer-derived best fits. The inset gives the k_i and k_i' values. Triangles, 2 mM CPIB; squares, 5 mM CPIB. Ordinate and abscissa as in Fig. 2.
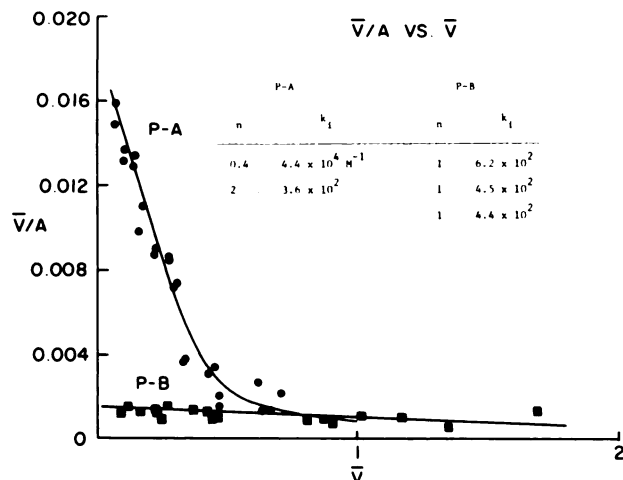
FIG. 4. *Binding of ^{14}C-chlorophenoxyisobutyrate to peptic fragments P-A and P-B*

Solid lines represent best fits, using the computer-derived k_i and k_i' values shown in the inset. Circles, fragment P-A; squares, fragment P-B.

helical measurements showing that the percentage of α-helix decreases from 57 to 42%. Fragment P-A also shows a loss of secondary structure, and reports have documented a certain loss of α-helical structure in both peptic fragments (10). It is probable that the lower affinities of both peptic fragments for ligands are associated with a loss of secondary structure. There is no evidence, however, that the small differences in α-helical content of P-A and P-B (48 vs 42%) are related to the large differences in association constants of the various ligands for these fragments. While absolute ligand affinities may be compromised in P-A and P-B, the simplest explanation of the data is that the high-affinity site for the ligands examined is found on one half of the molecule, and the low-affinity sites on the other half.

It is not clear whether the concept that the COOH-terminal half contains the high-affinity site for anions
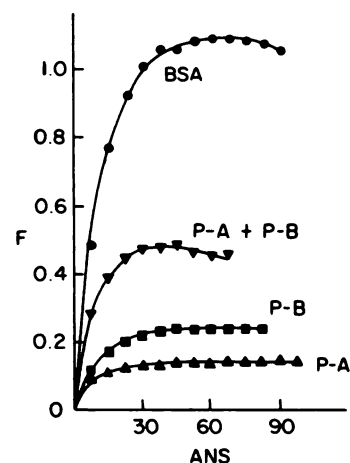

FIG. 6. *Titration of ANS fluorescence with BSA and peptic fragments*

Protein concentrations were 1×10^{-6} M. Fluorescence was measured at 37°C in an Eppendorf fluorimeter, with the excitation filter at 313–366 nm and emission at 400–3000 nm. Circles, half-cystinyl BSA; triangles, fragment P-A; squares, fragment P-B; inverted triangles, 1:1 molar ratio of P-A and P-B. Ordinate, fluorescence in arbitrary units. Abscissa, total ANS, $\times 10^{-6}$ M.

applies to human albumin as well. This protein, with 585 amino acid residues (2), is quite refractory to cleavage into fragments capable of ligand binding (5, 6) for reasons that are as yet unknown.

"Reconstitution" experiments, in which equimolar amounts of fragments P-A and P-B were mixed together, yielded a complex having the same α-helical content as the fragments. The binding affinities in the reconstituted particles were close to that expected from contributions of the individual association constants of P-A and P-B, as determined by quantitative comparison. On the other hand, King (4) reported that octanoate binds to the complex more tightly than expected, based on a summation of binding. Reed *et al.* (12) showed a twofold increase in binding of tryptophan and ANS to the 1:1
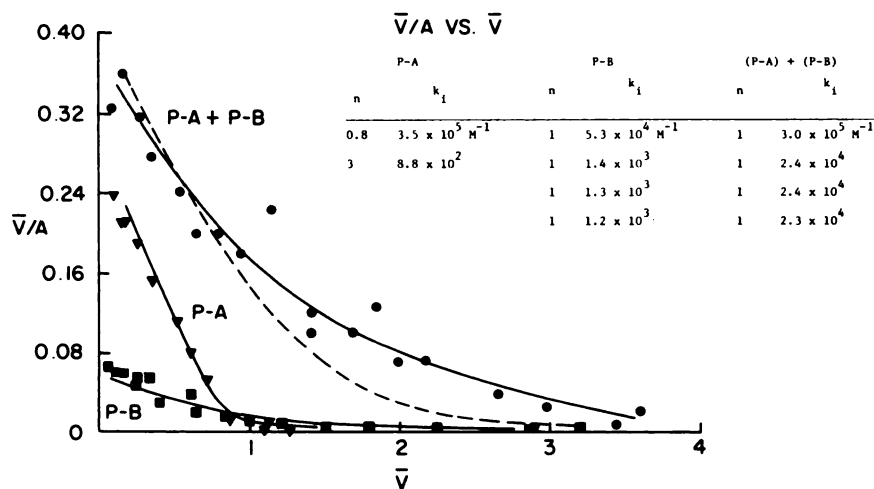

FIG. 5. *Binding of ^3H-ANS to peptic fragments P-A and P-B and reconstituted albumin*

Solid lines represent best fits, using an n_1 of 0.8 for fragment P-A. The inset gives the computer-derived k_i estimates. The dashed line is the simulated fit obtained by adding the experimentally derived k_i's of P-A and P-B. Ordinate, bound/free ^3H-ANS ($\times 10^6$ M); abscissa, moles ^3H-ANS bound/mole protein. Triangles, fragment P-A; squares, fragment P-B; circles, a 1:1 molar ratio of P-A and P-B. Protein concentration in all cases is 0.05 mM.

TABLE 2

Association constants of chlorophenoxyisobutyrate, 8-anilino-1-naphthalene sulfonate, and palmitate to BSA and peptic fragments

Association constants (k_i) were obtained from the computer-fitting programs, using either the site-binding equation, where $n = 1$, or the degenerate form, where sites are grouped into classes.

	Chlorophenoxyiso-butyrate		Anilinonaphthal-ene sulfonate		Palmitate	
	n	k	n	k	n	k
BSA	1	1.0×10^5 M^{-1}	1	6.8×10^5 M^{-1}	1	1.2×10^7 M^{-1}
	1	3.9×10^3	1	6.0×10^4	1	1.0×10^6
	1	1.8×10^3	1	1.1×10^4	1	9.6×10^5
	1	1.3×10^3	1	1.0×10^4	1	9.0×10^5
	1	1.0×10^3	1	1.7×10^0	1	8.5×10^5
P-A	0.4	4.4×10^4	0.8	3.5×10^5	0.8	8.0×10^6
	2	3.6×10^2	3	8.8×10^2	3	3.5×10^4
P-B	1	6.2×10^2	1	5.3×10^4	1	2.0×10^6
	1	4.5×10^2	1	1.4×10^3	1	1.8×10^5
	1	4.4×10^2	1	1.3×10^3	1	1.6×10^5
			1	1.2×10^3		

complex, as measured by fluorescence, at a fixed ligand concentration. However, several reports, including the present study, have demonstrated that such changes in fluorescence intensity are not proportional to changes in ligand binding (14, 29). Therefore, although the reconstituted fragments are bound tightly together with association constants of about 10^4 M^{-1} (12), our data provide no evidence of conformational change, measured by either circular dichroism or ligand binding.

Competitive interactions. We have discussed elsewhere the concept that a weaker binding ligand can displace a stronger ligand from whole albumin in an apparently competitive manner (14, 22, 25), but with unequal k_i and k_i' values. This analysis has been extended to the interaction between ^{14}C-palmitate and the competing anion octanoate or CPIB with peptic fragments. In either fragment, the weaker bound ligand displaced ^{14}C-palmitate, with apparent competition constants of about 10^{-1} less than the respective association constants. The fact that unequal k_i and k_i' values for certain ligand pairs are observed in peptic fragments as well as whole BSA is consistent with the view that no major cooperative interactions between halves of the albumin molecule are responsible for these differences. The data showing FFA displacement from either fragment are not consistent with the concept of different drug and FFA binding sites (30). Rather, the same sites that exist in whole albumin appear to be present in both fragments for strong and weak ligands, differing only in the affinity for the particular ligand.

ACKNOWLEDGMENTS

REFERENCES

1. Spector, A. Fatty acid binding to plasma albumin. *J. Lipid Res.* **16**: 165–179 (1975).
2. Brown, J. *Albumin Structure, Function, and Uses* (Rosenoer, Oratz, and Rothschild, eds.). Pergamon Press, New York, London, 27–52 (1977).
3. Bloomfield, V. The structure of bovine serum albumin at low pH. *Biochemistry* **5**: 684–691 (1966).
4. King, T. Limited pepsin digestion of bovine plasma albumin. *Arch. Biochem. Biophys.* **156**: 509–520 (1973).
5. Geisow, M., and G. Beaven. Large fragments of human serum albumin. *Biochem. J.* **161**: 619–625 (1977).
6. Heaney-Kieras, J., and T. King. Limited pepsin digestion of human plasma albumin. *J. Biol. Chem.* **252**: 4326–4329 (1977).
7. Feldhoff, R., and T. Peters. Fragments of bovine serum albumin produced by limited proteolysis. Isolation and characterization of peptic fragments. *Biochemistry* **14**: 4508–4514 (1975).
8. Markus, G., D. McClintock and B. Castellani. Tryptic hydrolysis of human serum albumin. The pattern of initial fragmentation. *J. Biol. Chem.* **242**: 4395–4401 (1967).
9. Peters, T., and R. Feldhoff. Fragments of bovine serum albumin produced by limited proteolysis. Isolation and characterization of tryptic fragments. *Biochemistry* **14**: 3384–3391 (1975).
10. Reed, R., R. Feldhoff, O. Clute and T. Peters. Fragments of bovine serum albumin produced by limited proteolysis. Conformation and ligand binding. *Biochemistry* **14**: 4578–4583 (1975).
11. Jusko, W., and M. Gretch. Plasma and tissue protein binding of drugs in pharmacokinetics. *Drug Metab. Rev.* **5**: 43–140 (1976).
12. Reed, R., R. Feldhoff and T. Peters. Fragments of bovine serum albumin produced by limited proteolysis: Complementary behavior of the large fragments. *Biochemistry* **15**: 5394–5398 (1976).
13. Jacobson, C. Lysine residue 240 of human serum albumin is involved in high-affinity binding of bilirubin. *Biochem. J.* **171**: 453–459 (1978).
14. Meisner, H., J. Stair and K. Neet. Quantitative assessment of the competitive binding of anionic ligands to albumin. *Mol. Pharmacol.* **18**: 230–236 (1980).
15. King, T., and M. Spencer. Structural studies and organic ligand-binding properties of bovine plasma albumin. *J. Biol. Chem.* **245**: 6134 (1970).
16. Foster, J. Plasma albumin, in *The Plasma Proteins*, Vol. 1 (F. Putnam, ed.). Academic Press, New York, 179–233 (1960).
17. Laemmli, U., E. Molbert, M. Showe and E. Kellenberger. Form-determining function of the genes required for the assembly of the head of bacteriophage T4. *J. Mol. Biol.* **49**: 99–113 (1970).
18. Chen, Y-H., J. Yang and H. Martinez. Determination of the secondary structures of proteins by circular dichroism and optical rotary dispersion. *Biochemistry* **11**: 4120 (1972).
19. Hartley, B. Strategy and tactics in protein chemistry. *Biochem. J.* **119**: 805–822 (1970).
20. Ambler, R. Enzymatic hydrolysis with carboxy peptidases. *Methods Enzymol.* **25**: 143–154 (1972).
21. Scatchard, G. The attraction of proteins for small molecules and ions. *Ann. N. Y. Acad. Sci.* **51**: 660–672 (1949).
22. Meisner, H., and K. Neet. Competitive binding of long chain free fatty acids, octanoate, and chlorophenoxyisobutyrate to albumin. *Mol. Pharmacol.* **14**: 337–346 (1978).
23. Ferguson, R., H. Edelhoch, H. Saroff and J. Robbins. Negative cooperativity in the binding of thyroxine to human serum prealbumin. *Biochemistry* **14**: 282–289 (1975).
24. Goodman, D. The interaction of human serum albumin with long chain fatty acid anions. *J. Am. Chem. Soc.* **80**: 3892–3898 (1958).
25. Meisner, H. Displacement of free fatty acids from albumin by chlorophenoxyisobutyrate. *Mol. Pharmacol.* **13**: 224–231 (1977).
26. Ho, R. Radioachemical assay of long chain fatty acids using ^{63}Ni as tracer. *Anal. Biochem.* **36**: 105–113 (1970).
27. Chen, R. Removal of fatty acids from serum albumin by charcoal treatment. *J. Biol. Chem.* **242**: 173–181 (1967).
28. Geisow, M., and G. Beaven. Physical and binding properties of large fragments of human serum albumin. *Biochem. J.* **161**: 477–484 (1977).
29. Santos, E., and A. Spector. Effect of fatty acids on the inteaction of 1-anilino-8-napthalene sulfonate with human plasma albumin. *Biochemistry* **11**: 2299–2304 (1972).
30. Birkett, D., S. Myers and G. Sudlow. Effect of fatty acids on two specific drug binding sites on human serum albumin. *Mol. Pharmacol.* **13**: 987–992 (1977).